PHYSICAL REVIEW D **86,** 074010 (2012)

# Probing new physics via $pp \to W^+W^- \to l\nu jj$ at the CERN LHC

Shuai Liu,[1] Yajun Mao,[1] Yong Ban,[1] Pietro Govoni,[2,3,4] Qiang Li,[1] Chayanit Asawatangtrakuldee,[1] and Zijun Xu[1]

[1]*Department of Physics and State Key Laboratory of Nuclear Physics and Technology, Peking University, Beijing 100871, China*
[2]*Milano-Bicocca University, Milano 20126, Italy*
[3]*INFN Milano-Bicocca, Milano 20126, Italy*
[4]*European Organization for Nuclear Research, Geneva CH-1211, Switzerland*

(Received 1 August 2012; published 8 October 2012)

TeV scale new physics, e.g., large extra dimensions or models with anomalous triple vector boson couplings, can lead to excesses in various kinematic regions on the semileptonic productions of $pp \to WW \to l\nu jj$ at the CERN LHC, which, although suffer from large QCD background compared with the pure leptonic channel $pp \to WW \to l\nu l\nu$, can benefit from larger production rates and the reconstructable four-body mass $M_{l\nu jj}$. We study the search sensitivity through the $l\nu jj$ channel at the 7 TeV LHC on relevant new physics via probing the hard tails on the reconstructed $M_{l\nu jj}$ and the transverse momentum of leptonically decayed $W$ boson ($P_{TW}$), taking into account main backgrounds and including the parton shower and detector simulation effects. Our results show that with integrated luminosity of 5 fb$^{-1}$, the LHC can already discover or exclude a large parameter region of the new physics, e.g., a 95% C.L. can be set on the large extra dimensions with a cutoff scale up to 1.5 TeV, and the $WWZ$ anomalous coupling down to, e.g., $|\lambda_Z| \sim 0.1$. Results are also given for the 8 TeV LHC.

DOI: 10.1103/PhysRevD.86.074010 PACS numbers: 13.85.Hd, 12.60.Cn, 14.70.Fm, 14.80.Rt

## I. INTRODUCTION

The Large Hadron Collider (LHC) had been running successfully during the 2010 and 2011 data taking period with the c.m. energy of 7 TeV, accumulating about 5 fb$^{-1}$ of data, and has been upgraded to 8 TeV and higher instantaneous luminosity [1], accumulating already another amount of data over 10 fb$^{-1}$. It has already enriched greatly our knowledge of electroweak symmetry breaking (especially the Higgs mechanism with the recent discovery of a 125–126 GeV Higgs-like boson [2,3]), the Standard Model (SM) precise measurement, SUSY, and extra dimension physics, etc. (see, e.g., Refs. [4–8]).

Taking the large extra dimensions (ADD) [9] as an example, searches have been performed on virtual-graviton channels at HERA [10,11], LEP [12–17], and the Tevatron [18,19]. The most stringent collider limits before the LHC were given by the Tevatron D0 through the dijet [20], diphoton, and dielectron channels [19], which excluded the ADD cutoff scale $M_s$ up to 1.3–2.1 TeV at a 95% C.L., for seven to two extra dimensions. Recently, ATLAS and CMS have updated these limits. The 95% C.L. from ATLAS read as 2.27–3.53 TeV depending on extra dimension number $\delta$ through diphoton search with integrated luminosity of 2.12 fb$^{-1}$ [21], while CMS gives 2.5–3.8 TeV and 2.3–3.8 TeV through diphoton [22,23] and dilepton searches [24],[1] respectively, with an integrated luminosity of about 2 fb$^{-1}$.

On the other hand, searches via gauge boson pair productions have also been proposed in various Refs. [26–30]. The corresponding characteristic signal shows as excesses on the transverse momentum ($P_T$) of either gauge boson or lepton invariant mass ($M_{VV}$) or transverse mass ($M_T$) of the gauge boson pair. Although the cross sections in both the SM and ADD are smaller than in the diphoton and dilepton channels, preliminary analyses [26,30] through the study of the $WW$ channel (without parton shower and detector simulation applied yet) show that $3\sigma$ sensitivity can be achieved for $M_s$ up to about 2 TeV and 4 TeV, with the integrated luminosity of 1 fb$^{-1}$ and 100 fb$^{-1}$ at the 7 TeV LHC, respectively. Needless to say, the search via diboson channel may also be used in combination with other analysis results to enlarge further the exclusion limits or discovery sensitivity.

In the meantime, digauge boson channels are also crucial for probing the triple gauge boson anomalous coupling (TGC), which have similar signal type as described above for the ADD and thus can be considered in the same study. So far the tightest cut on the TGC parameter, e.g., $\lambda_Z$ (which is the most interesting one for us to show here as an example to verify our MC estimation results in this paper, as it is relatively independent from other TGC parameters), is from Tevatron D0 with the resulted 95% C.L. as $-0.075 < \lambda_Z < 0.093$ [31], taking the form factor scale $\Lambda = 2$ TeV from measurement of $WZ \to l\nu ll$ with 4.1 fb$^{-1}$ of data. As for the $WW$ channel, which is of our interest, D0 gives $-0.10 < \lambda_Z < 0.11$ through $l\nu jj$ analysis with 1.1 fb$^{-1}$ of data [32], and $-0.14 < \lambda_Z < 0.18$ through $l\nu l\nu$ analysis with 1 fb$^{-1}$ of data [33]. The ATLAS Technical Digest Report [34] also gave an estimate on the ability of the 14 TeV LHC, which can reach

[1]Searches with a monojet and missing transverse energy via graviton real emission have also been performed at CMS with 36 pb$^{-1}$ of data [25], which, however, lead to rather loose limits at 95% C.L., i.e., 1.68–2.56 TeV for $\delta = 6$ to 2.

 © 2012 American Physical Society

$-0.028 < \lambda_Z < 0.024$ with 1 fb$^{-1}$ of data by fitting $M_T(WZ)$ in the $WZ$ measurement, and $-0.108 < \lambda_Z < 0.111$ from the $WW \to l\nu l\nu$ channel. Note also that recently ATLAS gave constraints as $-0.090 < \lambda_Z < 0.086$ for $\Lambda = 3$ TeV with 1.02 fb$^{-1}$ of data by fitting the $P_T$ of the leading lepton in the $WW \to l\nu l\nu$ measurement [35].

In this paper, we are interested in simulating and exploring the ability of new physics searches via the semileptonic channel of di-$W$ boson productions, i.e., $PP \to WW \to l\nu jj$, for both the ADD and TGC searches the LHC. The semileptonic channel, although it suffers from larger QCD background compared with the pure leptonic channel, can benefit from larger production rates and the reconstructable four-body mass $M_{l\nu jj}$, which can then be exploited for shape fitting in data analysis to control the background systematics via an extrapolation method from the control to signal region. Note the semileptonic $l\nu jj$ channel has already been studied extensively both in MC and experimental analysis on Higgs search [36–38] and triple gauge boson anomalous coupling [32], etc., which shows benefits to increase the search sensitivity either alone or by combining with other channels.

This paper is organized as follows. In Sec. II we list the signal and main backgrounds. In Sec. III we describe the simulation working line. In Sec. IV we present numerical results and their discussions. Finally we conclude in Sec. V.

## II. SIGNALS AND BACKGROUNDS

We show in Fig. 1 examples of relevant Feynman diagrams for $pp \to W^+W^- \to l\nu jj$ productions at the LHC. Additional contributions from the TGC and Kaluza-Klein (KK) gravitons in the ADD are represented by the bold vertex and line, respectively. Note in the ADD, Feynman diagrams from the gluon-gluon initial state channel also appear, while in the TGC, $pp \to WZ \to l\nu jj$ contributes in addition.

In the ADD model, there are infinite KK modes of gravitons. For virtual graviton channels, the summation over their propagators leads, however, to ultraviolet divergences. This happens because ADD is an effective theory, which is only valid below an effective energy scale. There are several popular ways of parametrizing the LO differential cross sections, including the Han, Lykken, Zhang [39], the Giudice, Rattazzi, Wells (GRW) [40], and the Hewett [41] conventions. In the following, we stick to the GRW one which does not depend on $\delta$, in which the summation over the KK graviton propagators can be approximated by

$$\frac{-1}{\bar{M}_{Pl}^2} \sum_{\vec{n}_\delta} \frac{1}{s - m_{\vec{n}_\delta}^2} = \frac{4\pi}{M_s^4}, \tag{2.1}$$

with $\bar{M}_{Pl}$ as the Planck scale and $\vec{n}_\delta$ is a $\delta$-dimension array representing the $n$th KK mode. In the GRW convention, the above-mentioned CMS analyses [22–24] set a 95% C.L. on $M_s$ up to about 3 TeV (with some differences depending on the choice of the next-to-leading order QCD K factor). Moreover, we will also present the results with a hard truncation scheme by setting the cut on the partonic center-of-mass energy

$$\sqrt{\hat{s}} < M_s. \tag{2.2}$$

As for the TGC, in this paper we are focusing on the $\lambda_Z$ term as in the following effective Lagrangian [42]:

$$\mathcal{L}_{\text{eff}}^{WWZ} \sim -ie \cot\theta_W \frac{\lambda_Z}{M_W^2} W_\mu^{+\nu} W_\nu^{-\rho} Z_\rho^\mu, \tag{2.3}$$

where $\theta_W$ is the weak mixing angle, and in the SM one has $\lambda_Z = 0$. Moreover, in order to avoid unitarity violation, we take the following commonly used dipole form factor:

$$\lambda_Z \to \frac{\lambda_Z}{(1 + \hat{s}/\Lambda^2)^2}, \tag{2.4}$$

with $\hat{s}$ as the gauge boson pair invariant mass and the parameter $\Lambda$ is fixed to be 2 TeV.

We have used MadGraph/MadEvent [43,44] to deal with the ADD and TGC models. As for the ADD, we have exploited previous implementation of spin-2 particles [45], but now with additional modifications on relevant HELAS subroutines [46] to realize the GRW summation convention, i.e., Eq. (2.1). For the TGC, we have used the FeynRules [47]-UFO [48]-ALOHA [49] framework to achieve its implementation within MadGraph/MadEvent. The unitary restoration formula Eq. (2.4) is realized by modifying MadEvent [50].

In Fig. 2, we show the $M_{WW}$ and $P_{TW}$ differential distributions for $pp \to W^+W^-$ (without $W$ decay) at the parton level, for the SM, the TGC with $\lambda_Z = 0.1$, and ADD with $M_s = 1.5$ and 1.8 TeV, with the total cross sections as 28.75, 29.34, 30.63, and 29.3 pb, respectively. Those results are for the 7 TeV LHC, and the renormalization/factorization scales are set to $\mu_r = \mu_f = \sqrt{P_{TW}^2 + M_W^2}$. One can see that both ADD and TGC lead to excesses on the hard tails of the $M_{WW}$ and $P_{TW}$ distributions: the

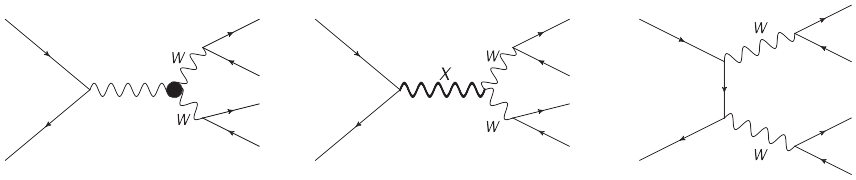


FIG. 1. Examples of Feynman diagrams on $l\nu jj$ productions at the LHC. The bold vertex and line represent the TGC and ADD Kaluza-Klein gravitons, respectively.

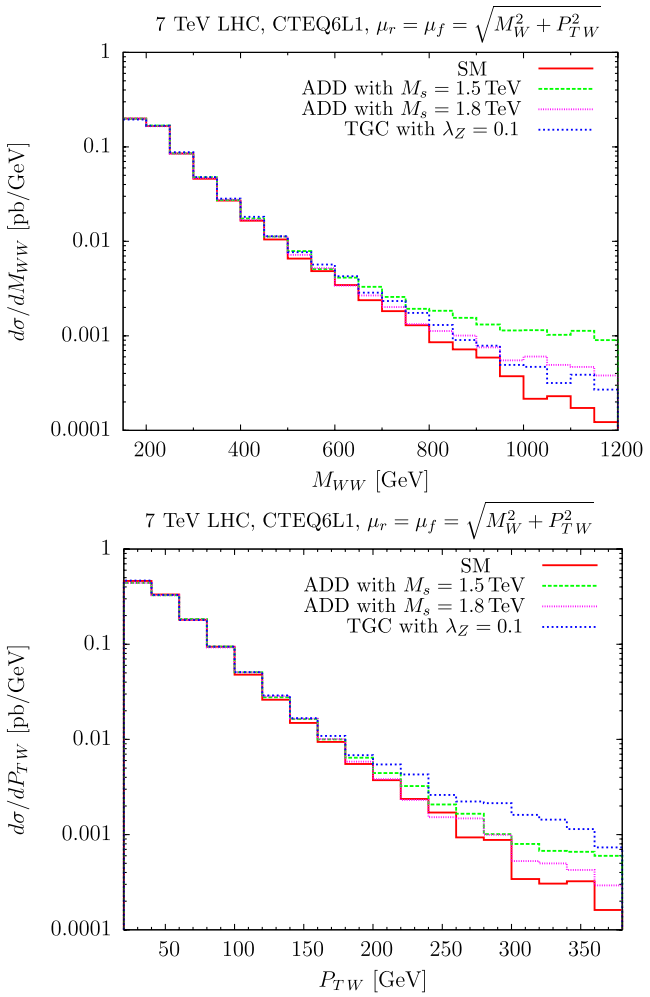


FIG. 2 (color online). Distributions on $M_{WW}$ and $P_{TW}$ for $pp \to W^+W^-$ at the parton level, for the SM, the TGC with $\lambda_Z = 0.1$, and ADD with $M_s = 1.5$ and 1.8 TeV.

ADD excesses appear from $M_{WW} \gtrsim 500$–$700$ GeV and $P_{TW} \gtrsim 200$–$250$ GeV for $M_s = 1.5$ and 1.8 TeV, yet the TGC excesses appear a bit earlier from $M_{WW} \gtrsim 400$ GeV and $P_{TW} \gtrsim 100$ GeV. One in principle can try to exploit the excesses to enlarge the signal over the background ratio to a large extent as one can, but to do that it needs a more realistic and complete simulation, taking into account acceptance efficiency, parton shower, and detector simulation effects, which will be discussed and shown in detail in the following.

The characteristic signal we are interested in contains one well-identified lepton (electron or muon) in association with large missing transverse energy $\not{E}_T$. The main background processes in the SM are listed as follows:

(1) $WW \to l\nu + jj$,
(2) $WZ \to l\nu + jj$,
(3) $WZ$, $ZZ \to jj + ll$ with one lepton misidentified,
(4) $W(\to l\nu)$ + 2-jets, which is the dominant background in our case,
(5) $Z(\to ll)$ + 2-jets with one lepton misidentified,
(6) $t\bar{t} \to l\nu jj + b\bar{b}$,
(7) $tW \to l\nu jj + b$,
(8) $tj \to l^+\nu j + b$,

where $l = e$, $\mu$ and $\tau$. Note that $\tau$ decays into $e$, $\mu$ at the ratio of about 35% and is handled with TAUOLA [51]. For (4), we have also compared the results with the one of matrix elements for $W + 1$, 2, 3 partons matched via PYTHIA6 [52] in the $k_T$-jet MLM scheme [53] implemented in MadGraph/MadEvent. In general, the matched results agree well with the $W + 2$-jets one on shapes for reconstructed $M_{l\nu jj}$, for example, yet with an enhancement of a factor $k \sim 1.5$ at the hard tail. For simplicity, we still use the $W + 2$-jets sample in our study as it takes much less computing time and size to reach higher statistics. Moreover, we have omitted the QCD multijet backgrounds with jet faking lepton, which is important mostly for electron channel [37,54] and hard to simulate due to instrumental effects, but fortunately it is much smaller than the dominant $W + 2$-jets backgrounds [37,54].

## III. SIMULATION FRAMEWORK

As mentioned above, we use MadGraph/MadEvent for hard process generation with the default renomalization and factorization scales chosen as the transverse mass of the core process. The next-to-leading order or NNLO QCD $K$ factors are included later for normalization, taken from MCFM [55] or relevant literatures. In more detail from MCFM, we assign a $K$ factor of 1.52 for $WW$ productions [56], 1.67 for $WZ$ [56], 1.0 for $W/Z$ + 2-jets [57,58], 1.02 for $tW$ [59], and 0.8 for $tj$ [60]. According to Ref. [61], we assign a $K$ factor of 1.52 for $t\bar{t}$ production to normalize the MadGraph/MadEvent LO result to the up-to-date theoretical prediction. As for the $WW$ productions in the ADD model, we set the $K$ factor the same as in the SM $WW$ case (note, however, it could be a bit larger at the hard tail of $M_{WW}$ and $P_{TW}$ than the SM $K$ factor according to Refs. [28,29]).

The generated unweighted events at parton level are then interfaced with PYTHIA6 for parton showering and hadronization. The multiple interaction option is also switched on. The detector simulation is realized with the help of Delphes V2.0 [62], where we focus on the CMS detector at the LHC. Finally, the sample analysis is performed with the program package ExRootAnalysis [63] and ROOT [64].

## IV. NUMERICAL RESULTS

We choose the following preselection cuts to generate unweighted events at parton level with MadGraph/MadEvent to interface later with PYTHIA and Delphes:

(i) $P_{Tj} \geq 20$ GeV, $|\eta_j| < 5$ and $R_{jj} \equiv \sqrt{\Delta\eta_{jj}^2 + \Delta\phi_{jj}^2} > 0.3$,
(ii) $P_{Tl} \geq 10$ GeV, and $|\eta_l| < 3$,
(iii) $R_{jl} \equiv \sqrt{\Delta\eta_{l,j}^2 + \Delta\phi_{l,j}^2} > 0.3$,

TABLE I. Cut flow at the LHC with $\sqrt{s} = 7$ TeV and an integrated luminosity of 5 fb$^{-1}$.

| Cut | $WW$ | $WZ(l\nu jj)$ | $jjll$ | $Wjj$ | $Zjj$ | $t\bar{t}$ | tw | tj | ADD(1.5 TeV) |
|---|---|---|---|---|---|---|---|---|---|
| (A) | 22 265 | 3866 | 1451 | 2 824 837 | 257 506 | 443 210 | 6612 | 15 836 | 23 977 |
| (B) | 13 900 | 2637 | 879 | 1 673 215 | 149 344 | 147 350 | 3793 | 11 774 | 14 989 |
| (C) | 10 666 | 1995 | 663 | 912 832 | 82 501 | 104 754 | 2805 | 5987 | 10 911 |
| (D) | 4117 | 894 | 283 | 298 093 | 28 110 | 70 994 | 1672 | 1666 | 4270 |
| (E) | 2654 | 596 | 123 | 183 820 | 12 129 | 53 903 | 1191 | 1222 | 2789 |
| (F) | 2292 | 512 | 96 | 158 679 | 9868 | 42 494 | 947 | 1047 | 2374 |
| (G) | 2168 | 489 | 91 | 153 022 | 9558 | 23 834 | 623 | 614 | 2255 |

for the signals and backgrounds listed in Sec. II, where $\eta$ is the pseudorapidity and $\phi$ is the azimuthal angle around the beam direction. Note, however, for the backgrounds (3) $WZ$, $ZZ \to jj + ll$ and (5) $Z(\to ll)$ + 2-jets, we do not require any of the above cuts in order not to make bias on the misidentified leptons.

Tighter cuts are then imposed on the reconstructed objects in the Delphes settings cards

(i) $P_{Te,\mu} \geq 30$ GeV, and $|\eta_{e,\mu}| < 2.4$.

(ii) Jets are clustered according to the anti-$k_t$ algorithm with a cone radius $\Delta R = 0.6$.

Moreover, $P_{T,j} > 30$ GeV and $|\eta_j| < 5$ are required.

Other high-level cuts are set in the analysis step as follows:

(a) one and only one lepton passing the above requirements,

(b) two or three jets,

(c) Choose as $W$ products the pair of jets with invariant mass closer to the $W$ mass, and then require $|M_{jj} - M_W| < 40$ GeV,[2]

(d) $R_{lj} > 0.4$,

(e) $\not{E}_T > 30$ GeV,

(f) $M_T^W \equiv \sqrt{2P_{T,l}\not{E}_T(1 - \cos(\Delta\phi(l, \not{E}_T)))} > 40$ GeV, with $M_T^W$ defined as the transverse mass of the lepton and $\not{E}_T$.

In Table I, we list the event numbers after each step of the analysis cuts, for an integrated luminosity of 5 fb$^{-1}$ at the 7 TeV LHC, for both the signal and background processes, where we take the ADD model with $M_s = 1.5$ TeV as an example for the signal. The dominant backgrounds so far are the $W$ + 2-jets and $t\bar{t}$. The signal excess $S$ reads as (ADD − WW) and the resulting $S/\sqrt{B}$ is only about 0.2. Further cuts must be exploited to enlarge the sensitivity where hints lie in Fig. 2.

We further impose additional cuts on the following variables to optimize the signal background significance:

(i) $\phi_{l,j}$,

(ii) $\Delta\eta_{jj}$, where the two jets correspond to the ones gotten from above (C),

(iii) $P_{TW}$ for the leptonically decayed $W$,

(iv) $M_{l\nu jj}$.[3]

We note the cuts on $P_{TW}$ and $M_{l\nu jj}$ are inspired from the parton level results as shown in Fig. 2, as ADD and TGC lead to excesses at their hard tails. The cuts on $\phi_{l,j}$ and $\Delta\eta_{jj}$ are considered, due to the reason that the signals tend to have two close jets back to the lepton, especially in the highly boosted case, while for the QCD the background it is flatter.

In Figs. 3 and 4, we show the distributions on $M_{l\nu jj}$ and $P_{TW}$ at the 7 TeV LHC for various backgrounds and the signals in the ADD model, i.e., the ADD Model with $M_s$ as 1.5 TeV, 1.8 TeV, and the truncated ADD with 1.5 TeV. Similar as what we have already seen from the parton level results in Fig. 2, the ADD signals tend to have hard tail. With further cuts as $M_{l\nu jj} > 0.9$ TeV, $P_{TW} > 200$ GeV, $\phi_{l,j} > 0.8$, $|\Delta\eta_{jj}| < 2.5$, and the minimum of $|M_{jj} - M_W| < 20$ GeV, we get $B = 19.1$, while for 1.5 TeV ADD we have $S = 9.4$ and $S/\sqrt{B} = 2.15$. Thus, with about 4.15 fb$^{-1}$ it is already enough to reach a 95% C.L. exclusion limit. For 1.5 TeV truncated ADD, we have $S = 6.0$ and $S/\sqrt{B} = 1.37$. For $M_s$ at 1.8 TeV and above, the significance can only reach about 0.4. To get close to a 95% limit, one needs over 100 fb$^{-1}$ of data. Note that although the sensitivities via the $l\nu jj$ channel appear to be lower than the above-mentioned CMS ones [22–24] which set a 95% C.L. on $M_s$ up to about 3 TeV in the GRW convention, the $l\nu jj$ channel can still play a complementary role for further confirmation or improvement through combination.

In Figs. 5 and 6, we show similar results as in Figs. 3 and 4, but now for the TGC signals. With cuts as $M_{l\nu jj} > 500$ GeV, $P_{TW} > 200$ GeV, $\phi_{l,j} > 0.8$, $\Delta\eta_{jj} < 1.5$, and $0 < M_{jj} - M_W < 25$ GeV (note this is chosen to optimize the sensitivity through changing the relative weight

[2]Note the mass window cut here is kind of loose for a robust reason. As for the ADD and TGC, a different tightening requirement will be needed in the next step.

[3]The neutrino momentum is extracted by imposing the invariant mass of the lepton and neutrino to be $m_W$. In case there are two solutions for neutrino momentum, we choose the one with smaller $p_z$.

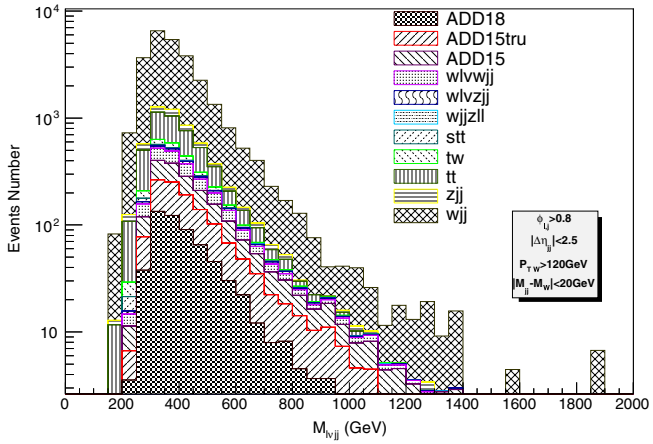


FIG. 3 (color online). $M_{l\nu jj}$ distributions for various backgrounds and the signals in the ADD model; i.e., the ADD model with $M_s$ as 1.5 TeV, 1.8 TeV, and the truncated ADD with 1.5 TeV, at the LHC with $\sqrt{s} = 7$ TeV and an integrated luminosity of 5 fb$^{-1}$.

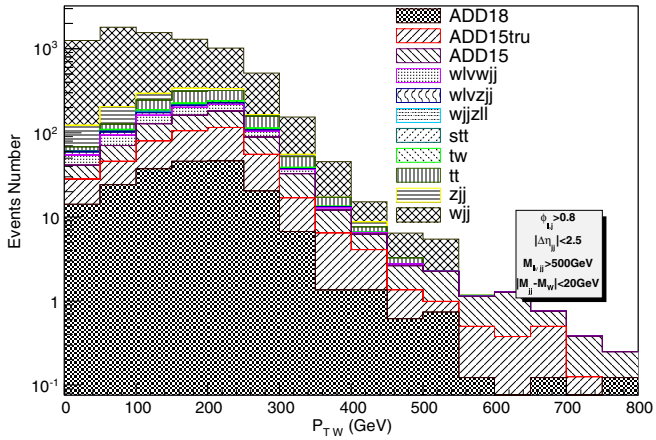


FIG. 4 (color online). $P_{TW}$ distributions for various backgrounds and the signals in the ADD model, at the LHC with $\sqrt{s} = 7$ TeV and an integrated luminosity of 5 fb$^{-1}$.

between the $WW$ and $WZ$ channel), we have $B = 452$, while for $\lambda_Z = 0.1$ TGC, we have $S = 40$ and thus $S/\sqrt{B} = 1.88$. For $\lambda_Z = -0.1$ TGC, we have $S = 44$ and $S/\sqrt{B} = 2.07$. For $\lambda_Z = 0.06$ TGC, we have $S = 14$ and $S/\sqrt{B} = 0.66$. We note these results are more or less near the ones in the ATLAS Technical Digest Report [34]

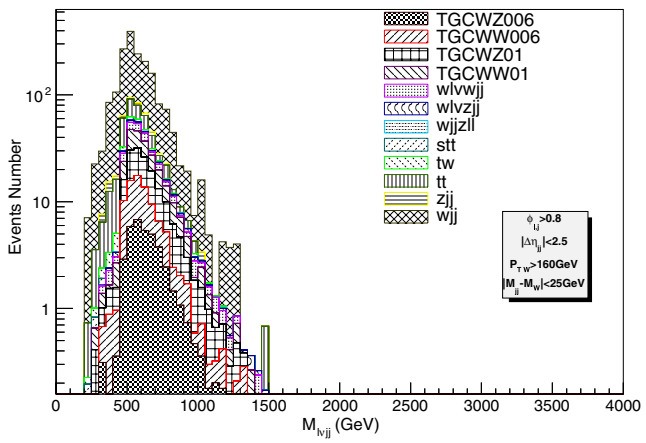


FIG. 5 (color online). $M_{l\nu jj}$ distributions for various backgrounds and the signals in the TGC model with $\lambda_Z = 0.06$ and 0.1 at the LHC with $\sqrt{s} = 7$ TeV and an integrated luminosity of 5 fb$^{-1}$.

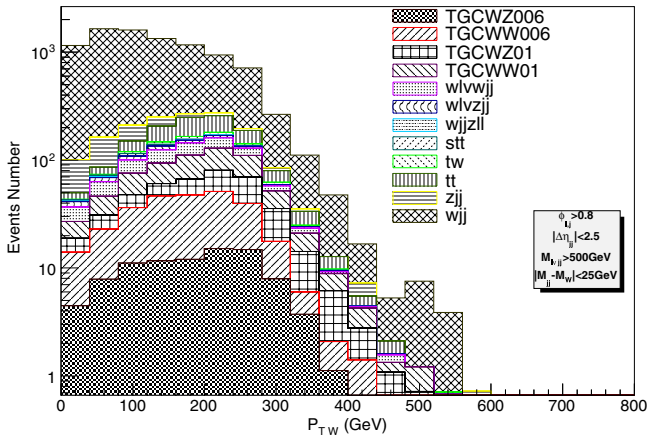


FIG. 6 (color online). $P_{TW}$ distributions for various backgrounds and the signals in the TGC model with $\lambda_Z = 0.06$ and 0.1 at the LHC with $\sqrt{s} = 7$ TeV and an integrated luminosity of 5 fb$^{-1}$.

where a 95% C.L. of $-0.108 < \lambda_Z < 0.111$ can be gotten from the $WW$ channel with 1 fb$^{-1}$ of data at the 14 TeV LHC, where the cross section for $WW$ processes, for example, gets increased by a factor of 3–4 compared with the 7 TeV LHC.

In Table II, we show the results of $S/\sqrt{B}$ for searching ADD with $M_s = 1.5$ TeV and 1.8 TeV, with or without

TABLE II. Sensitivity on ADD searches via the $WW \to l\nu jj$ channel at the LHC with $\sqrt{s} =$ 7 TeV and 8 TeV, respectively, and an integrated luminosity of 5 fb$^{-1}$. The corresponding uncertainty is also shown for simplicity just by enlarging or decreasing the background by a factor of 2.

| ADD | 1.5 TeV | 1.5 TeV Truncated | 1.8 TeV | 1.8 TeV Truncated |
|---|---|---|---|---|
| 7 TeV LHC | $2.15^{+0.89}_{-0.63}$ | $1.37^{+0.57}_{-0.40}$ | $0.37^{+0.12}_{-0.11}$ | $0.34^{+0.14}_{-0.10}$ |
| 8 TeV LHC | $2.22^{+0.92}_{-0.65}$ | $1.78^{+0.74}_{-0.52}$ | $0.61^{+0.25}_{-0.18}$ | $0.42^{+0.17}_{-0.11}$ |

truncation, at the LHC with $\sqrt{s} = 7$ TeV and 8 TeV, respectively. We also show the uncertainty of the significance for simplicity only by enlarging or decreasing the background by a factor of 2. However, we note here that the systematics can get controlled much better in relevant experimental analysis via the data driven method. While evaluating the numbers in the table, we set $\phi_{l,j} > 0.8$, $|\Delta\eta_{jj}| < 2.5$, and the minimum of $|M_{jj} - M_W| < 20$ GeV. For ADD with $M_s = 1.5$ TeV with or without truncation [Eq. (2.2)], we take further $M_{l\nu jj} > 0.9$ TeV and $P_{TW} > 200$ GeV. At the 8 TeV LHC, the sensitivities get larger compared with the 7 TeV LHC, especially for the larger $M_s$ case, which can reach 0.61 and 0.42 for $M_s = 1.8$ TeV, for example, with or without truncation.

## V. SUMMARY

In summary, we have presented here the first MC simulation study on searching the large extra dimensions via the $l\nu jj$ channel, taking into account the parton shower and detector simulation effects. We have also updated the results of probing triple gauge boson anomalous coupling through this same channel. Our results show that with only 5 fb$^{-1}$ of data, the 7 TeV LHC is sensitive to the large extra dimensions with energy scale at $M_s \sim 1.5$ TeV and the triple gauge boson anomalous coupling, e.g., $|\lambda_Z| \sim 0.1$. At the 8 TeV LHC, the sensitivities get further enhanced. For the larger $M_s(>1.8)$ TeV case, the LHC can only achieve the sensitivity at about the 0.4–0.5 level, which may be used for combining with other channels, e.g., the leptonic decay one as $l\nu l\nu$, and will be shown in our further works.

## ACKNOWLEDGMENTS

This work is supported in part by the National Natural Science Foundation of China, under Grants No. 10721063, No. 10975004, No. 10635030, and No. 11205008.

[1] http://cdsweb.cern.ch/journal/CERNBulletin/2012/06/News Articles/1423292?ln=en.
[2] F. Gianotti, CERN Seminar Report No. ATLAS-CONF-2012-093.
[3] J. Incandela, Update on the Standard Model Higgs Searches in CMS, CERN Seminar (CERN, unpublished).
[4] S. Chatrchyan *et al.* (CMS Collaboration), Phys. Lett. B **710**, 26 (2012).
[5] G. Aad *et al.* (ATLAS Collaboration), Phys. Lett. B **710**, 49 (2012).
[6] S. A. Koay (CMS Collaboration), EPJ Web Conf. **28**, 09008 (2012).
[7] P. de Jong, EPJ Web Conf. **28**, 09007 (2012).
[8] N. Vranjes (ATLAS Collaboration), Report No. ATL-PHYS-PROC-2012-040.
[9] N. Arkani-Hamed, S. Dimopoulos, and G. Dvali, Phys. Lett. B **429**, 263 (1998); I. Antoniadis, N. Arkani-Hamed, S. Dimopoulos, and G. Dvali, Phys. Lett. B **436**, 257 (1998); N. Arkani-Hamed, S. Dimopoulos, and G. Dvali, Phys. Rev. D **59**, 086004 (1999).
[10] C. Adloff *et al.*, H1 Collaboration, Phys. Lett. B **479**, 358 (2000).
[11] S. Chekanov *et al.*, ZEUS Collaboration, Phys. Lett. B **591**, 23 (2004).
[12] M. Acciarri *et al.*, L3 Collaboration, Phys. Lett. B **470**, 281 (1999).
[13] M. Acciarri *et al.*, L3 Collaboration, Phys. Lett. B **464**, 135 (1999).
[14] P. Abreu *et al.*, DELPHI Collaboration, Phys. Lett. B **485**, 45 (2000).
[15] P. Abreu *et al.*, DELPHI Collaboration, Phys. Lett. B **491**, 67 (2000).
[16] G. Abbiendi *et al.*, OPAL Collaboration, Eur. Phys. J. C **26**, 331 (2003).
[17] G. Abbiendi *et al.*, OPAL Collaboration, Eur. Phys. J. C **13**, 553 (2000).
[18] V. M. Abazov *et al.*, D0 Collaboration, Phys. Rev. Lett. **95**, 161602 (2005).
[19] V. M. Abazov *et al.*, D0 Collaboration, Phys. Rev. Lett. **102**, 051601 (2009).
[20] V. M. Abazov *et al.* (D0 Collaboration), Phys. Rev. Lett. **103**, 191803 (2009).
[21] G. Aad *et al.* (ATLAS Collaboration), Phys. Lett. B **710**, 538 (2012).
[22] S. Chatrchyan *et al.* (CMS Collaboration), J. High Energy Phys. 05 (2011) 085.
[23] S. Chatrchyan *et al.* (CMS Collaboration), arXiv: 1112.0688.
[24] S. Chatrchyan *et al.* (CMS Collaboration), Phys. Lett. B **711**, 15 (2012).
[25] S. Chatrchyan *et al.* (CMS Collaboration), Phys. Rev. Lett. **107**, 201804 (2011).
[26] J. Gao, C. S. Li, X. Gao, and J. J. Zhang, Phys. Rev. D **80**, 016008 (2009).
[27] N. Agarwal, V. Ravindran, V. K. Tiwari, and A. Tripathi, Nucl. Phys. **B830**, 248 (2010).
[28] N. Agarwal, V. Ravindran, V. K. Tiwari, and A. Tripathi, Phys. Rev. D **82**, 036001 (2010).
[29] N. Agarwal, V. Ravindran, V. K. Tiwari, and A. Tripathi, Phys. Lett. B **690**, 390 (2010).
[30] B. Yu-Ming, G. Lei, L. Xiao-Zhou, M. Wen-Gan, and Z. Ren-You, Phys. Rev. D **85**, 016008 (2012).
[31] V. M. Abazov *et al.* (D0 Collaboration), Phys. Lett. B **695**, 67 (2011).
[32] V. M. Abazov *et al.* (D0 Collaboration), Phys. Rev. D **80**, 053012 (2009).
[33] V. M. Abazov *et al.* (D0 Collaboration), arXiv:0907.4952.
[34] G. Aad *et al.* (ATLAS Collaboration), arXiv:0901.0512.

[35] G. Aad *et al.* (ATLAS Collaboration), Phys. Lett. B **712**, 289 (2012).
[36] T. Han and R.-J. Zhang, Phys. Rev. Lett. **82**, 25 (1999).
[37] S. Chatrchyan *et al.*, CMS Collaboration, CMS Physics Analysis Summary Report No. CMS PAS HIG-12-003, 2012.
[38] J. D. Lykken, A. O. Martin, and J.-C. Winter, J. High Energy Phys. 08 (2012) 062.
[39] T. Han, J. D. Lykken, and R. Zhang, Phys. Rev. D **59**, 105006 (1999).
[40] G. F. Giudice, R. Rattazzi, and J. D. Wells, Nucl. Phys. **B544**, 3 (1999).
[41] J. L. Hewett, Phys. Rev. Lett. **82**, 4765 (1999).
[42] K. Gaemers and G. Gounaris, Z. Phys. C **1**, 259 (1979); K. Hagiwara, K. Hikasa, R. D. Peccei, and D. Zeppenfeld, Nucl. Phys. **B282**, 253 (1987).
[43] J. Alwall, P. Demin, S. de Visscher, R. Frederix, M. Herquet, F. Maltoni, T. Plehn, D. L Rainwater, and T. Stelzer, J. High Energy Phys. 09 (2007) 028.
[44] J. Alwall, M. Herquet, F. Maltoni, O. Mattelaer, and T. Stelzer, J. High Energy Phys. 06 (2011) 128.
[45] K. Hagiwara, J. Kanzaki, Q. Li, and K. Mawatari, Eur. Phys. J. C **56**, 435 (2008).
[46] H. Murayama, I. Watanabe, and K. Hagiwara, Report No. KEK-Report 91-11, 1992 (unpublished).
[47] N. D. Christensen and C. Duhr, Comput. Phys. Commun. **180**, 1614 (2009).
[48] C. Degrande, C. Duhr, B. Fuks, D. Grellscheid, O. Mattelaer, and T. Reiter, Comput. Phys. Commun. **183**, 1201 (2012).
[49] P. de Aquino, W. Link, F. Maltoni, O. Mattelaer, and T. Stelzer, Comput. Phys. Commun. **183**, 2254 (2012).
[50] F. Maltoni and T. Stelzer, J. High Energy Phys. 02 (2003) 027.
[51] S. Jadach, J. H. Kühn, and Z. Was, Comput. Phys. Commun. **64**, 275 (1991); Report No. CERN-TH-5856-90.
[52] T. Sjostrand, L. Lonnblad, S. Mrenna, and P. Z. Skands, arXiv:hep-ph/0308153.
[53] J. Alwall, S. Hoche, F. Krauss, N. Lavesson, L. Lonnblad *et al.*, Eur. Phys. J. C **53**, 473 (2008).
[54] G. Aad *et al.*, ATLAS Collaboration, Phys. Rev. Lett. **107**, 231801 (2011).
[55] http://mcfm.fnal.gov/.
[56] J. M. Campbell, R. K. Ellis, and C. Williams, J. High Energy Phys. 07 (2011) 018.
[57] J. M. Campbell and R. K. Ellis, Phys. Rev. D **65**, 113007 (2002).
[58] J. M. Campbell, R. K. Ellis, and D. L. Rainwater, Phys. Rev. D **68**, 094021 (2003).
[59] J. M. Campbell and F. Tramontano, Nucl. Phys. **B726**, 109 (2005).
[60] J. M. Campbell, R. Frederix, F. Maltoni, and F. Tramontano, Phys. Rev. Lett. **102**, 182003 (2009).
[61] M. Cacciari, M. Czakon, M. L. Mangano, A. Mitov, and P. Nason, Phys. Lett. B **710**, 612 (2012).
[62] S. Ovyn, X. Rouby, and V. Lemaitre, arXiv:0903.2225.
[63] http://madgraph.hep.uiuc.edu/Downloads/ExRootAnalysis.
[64] R. Brun and F. Rademakers, Nucl. Instrum. Methods Phys. Res., Sect. A **389**, 81 (1997).